Aliphatic versus Aromatic C−H Activation in the Formation of Abnormal Carbenes with Iridium: A Combined Experimental and Theoretical Study

Mónica Viciano,[†] Marta Feliz,[‡] Rosa Corberán,[†] Jose A. Mata,[†] Eric Clot,*[,‡] and Eduardo Peris*[,†]

Departamento de Química Inorgánica y Orgánica, Universitat Jaume I, Avenida Vicente Sos Baynat s/n, 12071 Castellón, Spain, and Institut Charles Gerhardt, Université Montpellier 2, CNRS, cc 1501, Place Eugène Bataillon, 34000 Montpellier, France

Received July 12, 2007

The metalation of a series of C2-Me-substituted monoimidazolium and bisimidazolium salts to $[Cp^*IrCl_2]_2$ is described. The reaction of the monoimidazolium salt provides the species $Cp^*Ir(aNHC)Cl_2$, in which the NHC shows an abnormal coordination mode. The use of the bisimidazolium salt provides different reaction patterns depending on the linker length between the two azolium rings. For the methylene-linked bisimidazolium salt, the only compound obtained shows an unusual type of coordination in which the chelating ligand is coordinated through an abnormal NHC and a methylene group resulting from the CH activation of the C2-Me group. For the ethylene-linked bisimidazolium salt, a similar product is obtained, together with the chelating bis-abnormal-NHC species. All compounds have been fully characterized by usual spectroscopic techniques, and X-ray molecular structures are described. The formation of the reaction products, in the case of the methylene linker, has been rationalized by means of DFT calculations with inclusion of solvent effects (PCM). The calculations could not discriminate the nature of the first metalation between direct deprotonation of the ligand by the base and metalation through C−H activation at Ir. However both cases point to a kinetic preference for first metalation at the C2-Me group. The second metalation process is the result of kinetically preferred C−H activation at the C5 position.

Introduction

It is now well recognized that N-heterocyclic carbenes (NHCs) have provided new structural principles in the design of homogeneous catalysts,[1] and this has afforded the great development of NHC chemistry. A large number of examples reporting unprecedented and new topologies of coordinated ligands, effective catalytic responses in a wide variety of reactions, and new forms of bond activations are reported year after year.[2] Among these examples, those regarding the formation of abnormal carbenes and the design of compounds capable of activating selectively aromatic and aliphatic C−H bonds constitute fields in which N-heterocyclic carbenes have found a privileged position. Abnormal carbenes (NHC ligands bound through a backbone C4 or C5 carbon), first described by Crabtree and co-workers,[3] now constitute a new family of NHCs that are often found in the recent literature[4−8] and even have been reviewed.[9] The better σ-donor abilities of NHCs compared to phosphines facilitate C−H activation, and hence the number of papers regarding the intramolecular[10−15] and catalytic[14,16] versions of this process is continously increasing. Abnormal NHCs are considered more basic than normal NHCs,[4,5] so the

* Corresponding author. E-mail: eric.clot@univ-montp2.fr; eperis@qio.uji.es.

[†] Universitat Jaume I.

[‡] Université Montpellier 2.

(1) Herrmann, W. A.; Elison, M.; Fischer, J.; Kocher, C.; Artus, G. R. J. *Angew. Chem., Int. Ed. Engl.* **1995**, *34*, 2371.

(2) Peris, E.; Crabtree, R. H. *Coord. Chem. Rev.* **2004**, *248*, 2239. Crudden, C. M.; Allen, D. P. *Coord. Chem. Rev.* **2004**, *248*, 2247. Cesar, V.; Bellemin-Laponnaz, S.; Gade, L. H. *Chem. Soc. Rev.* **2004**, *33*, 619. Bourissou, D.; Guerret, O.; Gabbai, F. P.; Bertrand, G. *Chem. Rev.* **2000**, *100*, 39. Herrmann, W. A.; Kocher, C. *Angew. Chem., Int. Ed. Engl.* **1997**, *36*, 2163. Cavell, K. J.; McGuinness, D. S. *Coord. Chem. Rev.* **2004**, *248*, 671. Herrmann, W. A. *Angew. Chem., Int. Ed.* **2002**, *41*, 1291. Peris, E.; Crabtree, R. H. *C. R. Chim.* **2003**, *6*, 33. Mata, J. A.; Poyatos, M.; Peris, E. *Coord. Chem. Rev.* **2007**, *251*, 841.

(3) Grundemann, S.; Kovacevic, A.; Albrecht, M.; Faller, J. W.; Crabtree, R. H. *Chem. Commun.* **2001**, 2274.

(4) Appelhans, L. N.; Zuccaccia, D.; Kovacevic, A.; Chianese, A. R.; Miecznikowski, J. R.; Macchioni, A.; Clot, E.; Eisenstein, O.; Crabtree, R. H. *J. Am. Chem. Soc.* **2005**, *127*, 16299.

(5) Chianese, A. R.; Kovacevic, A.; Zeglis, B. M.; Faller, J. W.; Crabtree, R. H. *Organometallics* **2004**, *23*, 2461.

(6) Grundemann, S.; Kovacevic, A.; Albrecht, M.; Faller, J. W.; Crabtree, R. H. *J. Am. Chem. Soc.* **2002**, *124*, 10473. Stylianides, N.; Danopoulos, A. A.; Tsoureas, N. *J. Organomet. Chem.* **2005**, *690*, 5948.

(7) Kovacevic, A.; Grundemann, S.; Miecznikowski, J. R.; Clot, E.; Eisenstein, O.; Crabtree, R. H. *Chem. Commun.* **2002**, 2580. Hu, X.; Castro-Rodriguez, I.; Meyer, K. *Organometallics* **2003**, *22*, 3016. Graham, T. W.; Udachin, K. A.; Carty, A. J. *Chem. Commun.* **2006**, 2699. Hu, X. L.; Meyer, K. *J. Organomet. Chem.* **2005**, *690*, 5474.

(8) Alcarazo, M.; Roseblade, S. J.; Cowley, A. R.; Fernandez, R.; Brown, J. M.; Lassaletta, J. M. *J. Am. Chem. Soc.* **2005**, *127*, 3290.

(9) Arnold, P. L.; Pearson, S. *Coord. Chem. Rev.* **2007**, *251*, 596.

(10) Burling, S.; Mahon, M. F.; Powell, R. E.; Whittlesey, M. K.; Williams, J. M. J. *J. Am. Chem. Soc.* **2006**, *128*, 13702. Ampt, K. A. M.; Burling, S.; Donald, S. M. A.; Douglas, S.; Duckett, S. B.; Macgregor, S. A.; Perutz, R. N.; Whittlesey, M. K. *J. Am. Chem. Soc.* **2006**, *128*, 7452. Abdur-Rashid, K.; Fedorkiw, T.; Lough, A. J.; Morris, R. H. *Organometallics* **2004**, *23*, 86. Caddick, S.; Cloke, F. G. N.; Hitchcock, P. B.; Lewis, A. K. D. *Angew. Chem., Int. Ed.* **2004**, *43*, 5824. Dorta, R.; Stevens, E. D.; Nolan, S. P. *J. Am. Chem. Soc.* **2004**, *126*, 5054. Huang, J. K.; Stevens, E. D.; Nolan, S. P. *Organometallics* **2000**, *19*, 1194. Burling, S.; Mahon, M. F.; Paine, B. M.; Whittlesey, M. K.; Williams, J. M. J. *Organometallics* **2004**, *23*, 4537. Cabeza, J. A.; del Rio, I.; Miguel, D.; Sanchez-Vega, M. G. *Chem. Commun.* **2005**, 3956. Danopoulos, A. A.; Winston, S.; Hursthouse, M. B. *J. Chem. Soc., Dalton Trans.* **2002**, 3090. Hitchcock, P. B.; Lappert, M. F.; Terreros, P. *J. Organomet. Chem.* **1982**, *239*, C26. Cariou, R.; Fischmeister, C.; Toupet, L.; Dixneuf, P. H. *Organometallics* **2006**, *25*, 2126.

10.1021/om7006979 CCC: $37.00
Publication on Web 09/26/2007

use of the former ligands may favor processes involving C−H activation or, at least, may lead to unusual reactivity patterns.

We recently performed a series of experimental and theoretical studies aimed at understanding the mechanisms leading to the formation of a series of bis-chelating Ir−NHC complexes through intermolecular C−H activation.[17,18] We also described a series of Cp*Ir(NHC) complexes that undergo facile intramolecular C−H activation[14,15] and are effective catalysts in the deuteration of a wide range of organic molecules.[14] In our studies about the intramolecular C−H activation, we designed a series of experiments for elucidating the factors leading to either aromatic or aliphatic C−H activations.[15] Steric factors seemed to highly influence the process, although theoretical calculations are presently underway in order to support our conclusions.

In order to design selective C−H activation catalysts, it is important not only to understand both the steric and electronic influences of the ligands on the C−H activation processes, but also to understand the factors underlying selective metalation of the imidazolium ring at a given position. In this work, we describe the preparation of a series of abnormal-NHC complexes bound to a Cp*Ir fragment. The preparation of the monocarbenes and chelating biscarbenes leads to a series of complexes with unprecedented structural features. We describe a bis-abnormal-NHC and, more remarkably, an unexpected type of chelating abnormal-NHC in which the C−H activation of a C2-methyl group has occurred. DFT calculations (B3PW91) have been performed in order to elucidate the mechanism leading to the formation of the mixed system featuring both aliphatic and aromatic C−H activation.

Results and Discussion

Experimental Studies. To selectively prepare abnormal NHC complexes, one of the most convenient methods is to block the imidazolium ligand precursors by substitution at C2 with alkyl or aryl groups.[5,8,19] The coordination of 1,2,3-trimethylimidazolium iodide to $[Cp^*IrCl_2]_2$ was performed by transmetalation of the previously obtained silver-carbene in CH_2Cl_2 at 50 °C. The reaction product, **1**, was obtained in moderate yield (ca. 22%; Scheme 1).

Compound **1** was fully characterized by the usual spectroscopic techniques and elemental analysis. The spectroscopic data are consistent with the abnormal coordination of the NHC ligand. For example, the ^{1}H NMR spectrum shows the singlet due to the proton at C5 (δ 6.5), and the three signals due to the nonequivalent methyl groups of the azole ring (δ 3.77, 3.56, and 2.46). The ^{13}C NMR spectrum shows the signal due to the metalated carbene-carbon at δ 140.1, in the region where other abnormal Ir−NHCs appear.[4−6]

Scheme 1

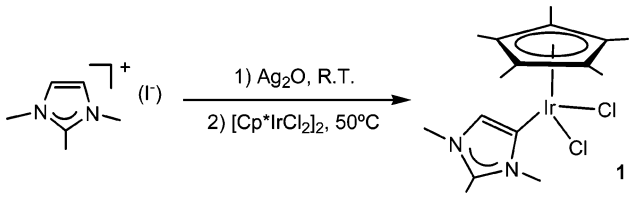

Scheme 2

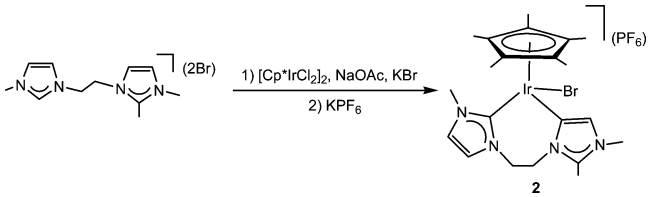

The recent preparation of 3-(2-Bromoethyl)-1-methylimidazolium bromide[20] affords a useful building block for the synthesis of unsymmetrical bisimidazolium salts. For example, the reaction of the latter compound with 1,2-dimethylimidazole allows the preparation of 1,1′-ethylene-2,3,3′-trimethylbis(1*H*-imidazolium) dibromide. This new biscarbene precursor offers the possibility of a chelating coordination in which the same ligand would simultaneously coordinate in normal and abnormal modes. The reaction of 1,1′-ethylene-2,3,3′-trimethylbis(1*H*-imidazolium) dibromide with $[Cp^*IrCl_2]_2$ in the presence of NaOAc in refluxing acetonitrile allows the preparation of compound **2**, in which the chelating-biscarbene ligand is coordinated by both the abnormal and normal modes (Scheme 2).

The most relevant features of the ^{1}H NMR spectrum of **2** are the signals due to the protons at the backbone of the normal (δ 7.01, 6.91) and abnormal (δ 6.26) coordinated azoles. The protons at the ethylene bridging group are diasterotopic at each carbon and hence appear as four different signals. The ^{13}C NMR spectrum shows the characteristic signals due to the normal (δ 152.7) and abnormal (δ 141.9) carbene carbons.

The molecular structure of **2** was unequivocally confirmed by means of X-ray diffraction studies. Figure 1 shows the ORTEP diagram of the molecule, together with the most relevant distances and angles.

The structure of the complex confirms that the chelating ligand is bound through both an abnormal and normal coordination of the NHC rings, with the formation of a seven-membered iridacycle. The Cp* ring and a bromine ligand complete the coordination sphere around the Ir center. The chelate bite angle is 92.7°, slightly larger than a previously reported chelating methylene-bridged bis-NHC.[21] The Ir−$C_{carbene}$ distances are 2.007 and 2.079 Å, corresponding to the normal[12−15,21,22] and abnormal carbenes,[4−6] respectively, and lie in the expected range for this type of bondings on related Ir(III) species. Interestingly, the longer Ir−C distance for the abnormal carbene lies closer to the range of related metalated Ir−aryl species,[14,15] suggesting that the bond may be considered as an extreme type of carbene,

(11) Scott, N. M.; Dorta, R.; Stevens, E. D.; Correa, A.; Cavallo, L.; Nolan, S. P. *J. Am. Chem. Soc.* **2005**, *127*, 3516. Scott, N. M.; Pons, V.; Stevens, E. D.; Heinekey, D. M.; Nolan, S. P. *Angew. Chem., Int. Ed.* **2005**, *44*, 2512.

(12) Prinz, M.; Grosche, M.; Herdtweck, E.; Herrmann, W. A. *Organometallics* **2000**, *19*, 1692.

(13) Hanasaka, F.; Tanabe, Y.; Fujita, K.; Yamaguchi, R. *Organometallics* **2006**, *25*, 826.

(14) Corberan, R.; Sanau, M.; Peris, E. *J. Am. Chem. Soc.* **2006**, *128*, 3974.

(15) Corberan, R.; Sanau, M.; Peris, E. *Organometallics* **2006**, *25*, 4002.

(16) Fructos, M. R.; Belderrain, T. R.; de Fremont, P.; Scott, N. M.; Nolan, S. P.; Diaz-Requejo, M. M.; Perez, P. J. *Angew. Chem., Int. Ed.* **2005**, *44*, 5284. Fructos, M. R.; de Fremont, P.; Nolan, S. P.; Diaz-Requejo, M. M.; Perez, P. J. *Organometallics* **2006**, *25*, 2237.

(17) Viciano, M.; Poyatos, M.; Sanau, M.; Peris, E.; Rossin, A.; Ujaque, G.; Lledos, A. *Organometallics* **2006**, *25*, 1120.

(18) Viciano, M.; Mas-Marza, E.; Poyatos, M.; Sanau, M.; Crabtree, R. H.; Peris, E. *Angew. Chem., Int. Ed.* **2005**, *44*, 444.

(19) Chianese, A. R.; Zeglis, B. M.; Crabtree, R. H. *Chem. Commun.* **2004**, 2176. Bacciu, D.; Cavell, K. J.; Fallis, I. A.; Ooi, L. L. *Angew. Chem., Int. Ed.* **2005**, *44*, 5282.

(20) Field, L. D.; Messerle, B. A.; Vuong, K. Q.; Turner, P. *Organometallics* **2005**, *24*, 4241.

(21) Vogt, M.; Pons, V.; Heinekey, D. M. *Organometallics* **2005**, *24*, 1832.

(22) Hanasaka, F.; Fujita, K.; Yamaguchi, R. *Organometallics* **2005**, *24*, 3422.

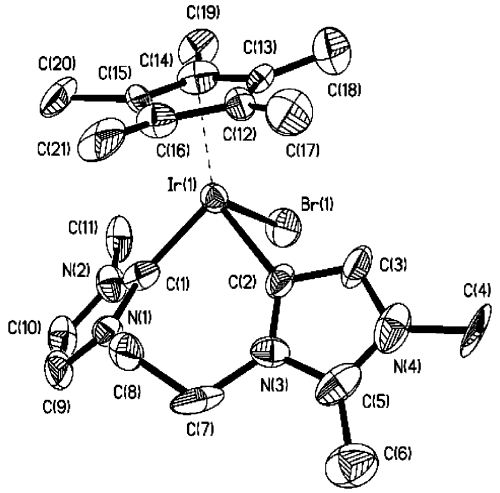

Figure 1. Molecular diagram of **2**. Ellipsoids are at 50% probability. Hydrogen atoms and counterion (PF_6) have been omitted for clarity. Selected bond distances (Å) and angles (deg): Ir(1)−C(1) 2.007 (12), Ir(1)−C(2) 2.079 (13), Ir(1)−Br(1) 2.5728 (18), C(1)−Ir(1)−C(2) 92.7(5).

Scheme 3

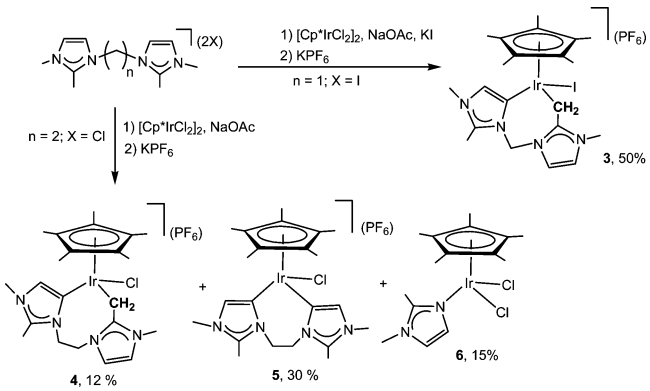

close in nature to a metalated aryl group. Other structural parameters are unexceptional.

With the aim of obtaining species related to **2**, but with bis-abnormal chelating ligands, we prepared the bis-imidazolium precursors 1,1′-methylenebis(2,2′,3,3′-tetramethylimidazolium) diiodide and 1,1′-ethylenebis(2,2′,3,3′-tetramethylimidazolium) dichloride. Almost simultaneously to our work (in fact during the editorial process of the present article), a similar methylene-bridged precursor was described and coordinated to Pd in a chelating bis-abnormal form.[23] With the use of the two different linkers, we wanted to study if there were any differences in reactivity due to ligand anisotropy, as we have observed for other examples.[17,24] As depicted in Scheme 3, both ligand precursors show significant differences when reacting with $[Cp^*IrCl_2]_2$. To our surprise, the reaction of 1,1′-methylenebis-(2,2′,3,3′-tetramethylimidazolium) diiodide with $[Cp^*IrCl_2]_2$ in refluxing acetonitrile in the presence of NaOAc yielded a major compound in which the ligand is coordinated in a chelating form through an abnormal carbene and a metalated methylene group (Scheme 3, compound **3**). The metalated methylene group comes from the C−H activation of the C2-Me group of the azolium

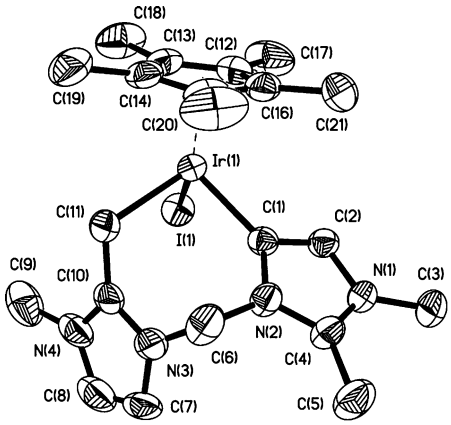

Figure 2. Molecular diagram of **3**. Ellipsoids are at 50% probability. Hydrogen atoms, crystallization solvent (CH_2Cl_2), and counterion (PF_6) have been omitted for clarity. Selected bond distances (Å) and angles (deg): Ir(1)−C(1) 2.047(3), Ir(1)−C(11) 2.149, Ir(1)−I(1) 2.7443(3), C(1)−Ir(1)−C(11) 97.04(14).

precursor. This product was the only detected species for this reaction, together with a small amount of unreacted $[Cp^*IrCl_2]_2$. When the ethylene-linked precursor 1,1′-ethylenebis(2,2′,3,3′-tetramethylimidazolium) dichloride was used, three different compounds were obtained: the chelating C2-Me-activated compound (**4**), the chelating-bis-abnormal-NHC product (**5**), and a new neutral species with a 1,2-dimethylimidazol ligand (**6**). Interestingly, the C2-Me-activated product **4**, was the minor species for the reaction with the ethylene-linked bis-NHC precursor.

All compounds **3**, **4**, **5**, and **6** were characterized by means of the usual spectroscopic techniques and elemental analysis. Both **3** and **4** display NMR spectra showing the loss of symmetry of the ligand upon coordination. The ^1H NMR spectra of **3** and **4** show the signals due to the nonequivalent geminal protons of the metalated CH_2 group (compound **3**, 4.23 and 3.22 ppm, $^2J_{H-H} = 11.7$ Hz; compound **4**, 3.72 and 2.60 ppm, $^2J_{H-H} = 13.6$ Hz). Three sets of singlets are observed due to the nonequivalent signals of the N-CH_3 and C2-Me methyl groups. The signals at −15 and 29 ppm in the ^{13}C NMR spectrum are assigned to the metalated carbon of the methylene group in **3** and **4**, respectively. The signals due to the abnormal carbene carbons appear at 146.0 (**3**) and 142.1 (**4**) ppm.

The NMR spectra of **5** show that the 2-fold symmetry of the ligand is maintained after its coordination to the metal. The protons at the C2-Me position display a signal at 2.54 ppm in the ^1H NMR spectrum. The ^{13}C NMR spectrum shows a signal at δ 141.1 attributed to the equivalent carbene abnormal carbon atoms.

The molecular structures of **3** and **5** were confirmed by X-ray diffraction studies. Figure 2 shows the ORTEP diagram of **3** and the most relevant distances and angles. The structure reveals that the ligand is coordinated in a bis-chelating form through an abnormal binding of the NHC and a methylene group, forming a distorted seven-membered iridacycle. A Cp* ring and a iodine ligand complete the coordination sphere around the metal center. The Ir−$C_{carbene}$ distance of 2.047 Å lies in the expected range of other Ir−NHC ligands with abnormal binding[4−6] and is also similar to that shown for compound **2** described in the present work. The Ir−CH_2 distance of 2.149 Å is similar to the distances shown by other iridium alkyl-cyclometalated species.[11,13,15]

Figure 3 shows the ORTEP diagram of compound **5**. The structure reveals that the coordination of the ligand is chelating,

(23) Heckenroth, M.; Kluser, E.; Neels, A.; Albrecht, M. *Angew. Chem., Int. Ed.* **2007**, *46*, 6293−6296.

(24) Mata, J. A.; Chianese, A. R.; Miecznikowski, J. R.; Poyatos, M.; Peris, E.; Faller, J. W.; Crabtree, R. H. *Organometallics* **2004**, *23*, 1253.

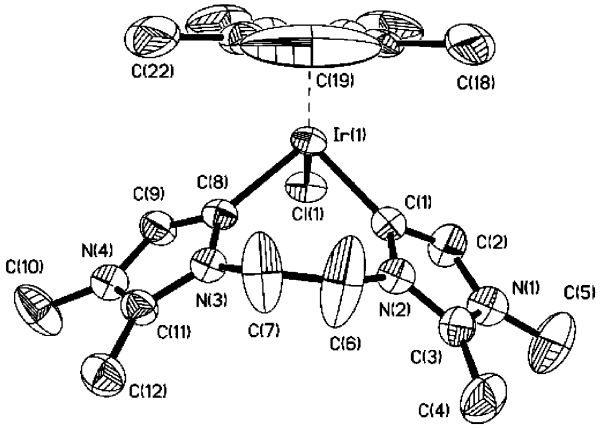

Figure 3. Molecular diagram of **5**. Ellipsoids are at 50% probability. Hydrogen atoms, two $CHCl_3$ molecules, and counterion (PF_6) have been omitted for clarity. Selected bond distances (Å) and angles (deg): Ir(1)−C(1) 2.039(7), Ir(1)−C(8) 2.039(6), C(1)−Ir(1)−C(8) 88.1(3).

with the two azole rings in an abnormal coordination mode. Both Ir−$C_{carbene}$ distances are 2.039 Å, in the range of other Ir−NHC ligands with abnormal binding.[4−6] The chelating ligand bite angle is 88.1°, slightly smaller than the angle shown in the related normal/abnormal bis-NHC compound **2** (92.7°), but this may be due to the higher steric size of the chlorine ligand in **5** compared to the bromine in **2**. All other structural parameters are unexceptional. The molecular structure of **6** was also confirmed by X-ray diffraction studies (Table 1 and Supporting Information).

While the field of C−H activation has witnessed significant advances in the last decade, there still lacks a series of general, selective, and efficient catalytical functionalization of unactivated sp^3 C−H bonds.[25] We recently reported that Cp*Ir(NHC) complexes can undergo facile intramolecular aromatic or aliphatic C−H activation reactions.[15] The nature of the C−H bond activated (aromatic vs aliphatic) depends on the sterics of the two R groups on the nitrogen atoms of the NHC ligand. The selectivity observed was considered to be steric in origin, even though calculations are presently underway to validate this hypothesis. However, in these systems, the first metalation is a straightforward coordination of a normal NHC ligand generated *in situ*.

C−H oxidative addition of imidazolium salts to transition metal complexes has been used as an alternative to the standard deprotonation by a strong base in the synthesis of NHC complexes bearing functionalities.[2] In some cases the C−H oxidative addition process was confirmed experimentally by the observation of a hydride bonded to the metal,[18,26] but most often the products obtained featured the NHC coordinated to the metal and no hydride was observed. However, there was always a weakly basic functionality present in the system. This could be an acetate ligand,[27] a hydride ligand,[3,4] a nitrogen atom in the reactant,[28] or even an added weak base (NR_3, AcO^-, or others).[15,17,21]

When bonded to the metal, the basic functionality has been shown computationally to promote C−H activation through a heterolytic bond cleavage pathway.[4,29] However, when an external base is added, the role of the latter remains an open question. It could deprotonate the imidazolium to generate the carbene ligand, which would coordinate easily to the metal, or it could deprotonate the metal once the C−H oxidative addition has been performed. Depending on the situation, the outcome of the reaction could be different, as the acidity of the various hydrogen atoms on the imidazolium does not necessarily correlate with the ease of C−H activation at the same sites. For imidazolium with a hydrogen atom at the C2 position, the acidity of the latter is significantly higher than those of the other sites, thus justifying that the metalation usually occurs at the C2 position. However, it was shown, both experimentally and computationally, that the outcome of the reaction may, in some cases, be influenced by the nature of the counteranion in the imidazolium salt.[4] Also DFT calculations showed that the activation barriers for C−H activation at the C2 and C5 positions were of similar magnitude,[4] despite the large difference in pK_a values.[30]

With bisimidazolium salts, two C−H activation processes are needed and the nature of the product is not necessarily easy to anticipate. When two C2−H bonds are present, the expected chelating normal biscarbene is obtained.[17] In that case, DFT calculations with NX_3 (X = H, Me, Et) as a model for the base could not determine the nature of the first metalation process (direct deprotonation at C2 or C2-H oxidative addition). The metalation of the second imidazolium moiety was shown to proceed exclusively through C−H oxidative addition with activation barriers of ca. 30 kcal mol^{-1} when the linker between the two imidazolium rings is CH_2. With a $(CH_2)_3$ linker the activation barriers were ca. 10 kcal mol^{-1} higher.

When metalation at the C5 position is sought, introducing a methyl group at the C2 position is the procedure generally used. In the present case such a strategy failed to yield the bis-abnormal carbene, and complex **3**, featuring an abnormal carbene and C−H activation of the methyl group, was obtained instead as the only product (Scheme 3). Only when the length of the linker between the two imidazoliums was increased from one to two methylene groups could the expected bis-abnormal isomer (**5**) be obtained together with the mixed system (**4**) and a complex resulting from degradation of the ligand (**6**). In order to shed more light on the process underlying the metalation of the imidazolium salt, DFT calculations were carried out at the B3PW91 level. Particular emphasis has been put on the determination of the mechanism for formation of **3**, while in the case of the longer linker the formation of the degradation product **6** was addressed.

DFT Studies of the Metalation of the Bisimidazolium. Mechanism for the Formation of 3. As we considered that the selective formation of **3** could be the result of the steric and/or electronic influence of the system used experimentally, calculations were carried out on the actual experimental systems Cp*IrI_2 and the bisimidazolium dication 1,1′-methylenebis-(2,2′,3,3′-tetramethylimidazolium), **bisIm**$^{2+}$, together with AcO^-

(25) Crabtree, R. H. *J. Organomet. Chem.* **2004**, *689*, 4083.
(26) McGuinness, D. S.; Cavell, K. J.; Yates, B. F. *Chem. Commun.* **2001**, 355.
(27) Peris, E.; Loch, J. A.; Mata, J.; Crabtree, R. H. *Chem. Commun.* **2001**, 201.
(28) Wiedemann, S. H.; Lewis, J. C.; Ellman, J. A.; Bergman, R. G. *J. Am. Chem. Soc.* **2006**, *128*, 2452.
(29) Garcia-Cuadrado, D.; Braga, A. A. C.; Maseras, F.; Echavarren, A. M. *J. Am. Chem. Soc.* **2006**, *128*, 1066. Davies, D. L.; Donald, S. M. A.; Macgregor, S. A. *J. Am. Chem. Soc.* **2005**, *127*, 13754. Davies, D. L.; Donald, S. M. A.; Al-Duaij, O.; Fawcett, J.; Little, C.; Macgregor, S. A. *Organometallics* **2006**, *25*, 5976. Davies, D. L.; Donald, S. M. A.; Al-Duaij, O.; Macgregor, S. A.; Polleth, M. *J. Am. Chem. Soc.* **2006**, *128*, 4210.
(30) Amyes, T. L.; Diver, S. T.; Richard, J. P.; Rivas, F. M.; Toth, K. *J. Am. Chem. Soc.* **2004**, *126*, 4366.

as the base. The reference, from which all energy values given in the figures thereafter are evaluated, is thus the globally neutral system {Cp*IrI_2, **bisIm**$^{2+}$, 2 AcO^-}. All the complexes to be described have been optimized at the B3PW91 level in the gas phase. As proton-transfer processes are compared to bond activation ones, the influence of the solvent (acetonitrile) was considered through PCM single-point calculations on gas-phase-optimized geometries (see Computational Details) and all the energy values given are PCM electronic energy values. No attempt was made to use Gibbs free energy values because no optimization within the PCM methodology was carried out, and using the corrections calculated in the gas phase on the PCM electronic energies was considered not to be accurate. Moreover, Gibbs free energies are generally important when comparison is made between steps of different molecularity. Here, processes to be compared have the same molecularity and differ only in the position of metalation. To clearly distinguish the activation processes at the cyclic sp^2 carbon or at the exocyclic sp^3 methyl one, the labels *vy* and *me* will be used, respectively.

The geometry of the dimer $[Cp^*IrI_2]_2$ was optimized, and the structural parameters (see Supporting Information) were in excellent agreement with the experimental data.[31] The reaction energy associated with the formation of the two Cp*IrI_2 monomers from the dimer is computed to be 7.0 kcal mol^{-1} at the PCM(B3PW91/CH_3CN) level, and this stabilization energy is not enough to compensate for the gain in entropy upon dissociation of the dimer (ca. −10 kcal mol^{-1}). Therefore the dimer is expected to be completely dissociated in acetonitrile, and the mechanistic studies will consider the monomer Cp*IrI_2 as the reactive complex.

The structures (and PCM energies with respect to the reference) for the transition states corresponding to the first C−H activation of **bisIm**$^{2+}$ at the methyl group (**TS1me**) or at the abnormal C5 position (**TS1vy**) are shown in Figure 4, together with the structure of the products before (**IrI$_2$meH**$^+$ and **IrI$_2$vyH**$^+$) and after deprotonation by the base AcO^- (**IrI$_2$me** and **IrI$_2$vy**). No adduct, in the form of σ- or π-complex, prior to C−H activation could be found on the potential energy surface (PES). The C−H activation at the methyl position is calculated to be easier than the C−H activation at the vinylic position by 2.5 kcal mol^{-1}. The geometries of both TS are typical of C−H activation processes with an elongated C−H bond (1.523 Å, **TS1me**; 1.314 Å, **TS1vy**), an almost formed Ir−C bond (2.338 Å, **TS1me**; 2.182 Å, **TS1vy**), and a short Ir···H contact (1.597 Å, **TS1me**; 1.676 Å, **TS1vy**). The deprotonation of the product of C−H activation (**IrI$_2$meH**$^+$ and **IrI$_2$vyH**$^+$) is calculated to be very exothermic because the conjugate bases (**IrI$_2$me** and **IrI$_2$vy**) are stable 18-electron Ir(III) complexes.

From these intermediates a vacant site is easily generated by dissociation of one iodine ligand to yield the dicationic 16-electron complexes **IrIme** and **IrIvy**. The iodine dissociation energies are 12.5 and 11.7 kcal mol^{-1}, respectively. Dissociation of I^- is easier in **IrI$_2$vy** because the abnormal carbene is expected to be a stronger donor than the alkyl group in **IrI$_2$me**, thus affording greater stabilization of the unsaturation at Ir. Note that the iodine dissociation from the 16-electron complex Cp*IrI_2 is calculated to be 37 kcal mol^{-1}, clearly showing the necessity to create first the metal−carbon bond before generating the vacant site needed for the second metal−carbon bond to be formed. From **IrIme** and **IrIvy** the transition states for C−H activation at the methyl position of the pending imidazolium

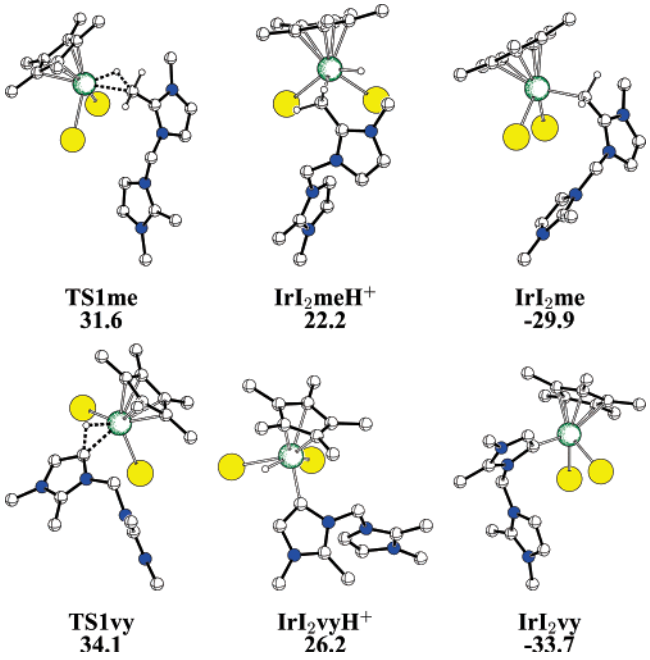

Figure 4. Optimized geometries and energies (kcal mol^{-1}, expressed relatively to the reference system, see text) along the first C−H activation process at the methyl position (top) and at the C5 position (bottom). Hydrogen atoms not involved in the reaction have been omitted for clarity. **IrI$_2$me** and **IrI$_2$vy** are monocationic, while the other complexes are dicationic.

group have been located on the potential energy surface (**TS2meme** and **TS2vyme**, respectively; see Figure 5). Even though an eight-membered metallacycle is formed in **TS2meme** and a seven-membered one in **TS2vyme**, the activation barriers for the C−H activation have similar values (24.6 kcal mol^{-1}, **TS2meme**; 23.9 kcal mol^{-1}, **TS2vyme**). Also, in both cases, the energies associated with the proton transfer to AcO^- are very close (−50.6 and −50.5 kcal mol^{-1}, respectively), pointing to similar acidities of the product of C−H activation, **IrImemeH**$^+$ and **IrvymeH**$^+$ (see Figure 5). However, despite the similarities of the processes to form **IrImeme** and **IrIvyme**, the latter is 5.7 kcal mol^{-1} more stable than the former as the result of the presence of a ligand with stronger donating abilities. As a matter of fact the intermediate **IrIvy** is 4.6 kcal mol^{-1} more stable than **IrIme**, and the increased stabilization of **IrIvyme** with respect to **IrImeme** (5.7 vs 4.6 kcal mol^{-1}) could be ascribed to the difference in stability between a seven-membered ring in **IrIvyme** and an eight-membered ring in **IrImeme**.

The process for C−H activation at the C5 position from **IrIme** and **IrIvy** was searched for and turned out to be a two-step process in both cases. The first step is associated with the coordination of the C4═C5 bond to Ir to yield the dicationic 18-electron complexes **IrIme_ene** and **IrIvy_ene**, respectively (Figure 6). The coordination is exothermic ($\Delta E = -5.5$ kcal mol^{-1}, **IrIme_ene**; $\Delta E = -1.9$ kcal mol^{-1}, **IrIvy_ene**), and the corresponding TSs (not shown in Figure 6) have been located; they are associated with low activation barriers (3.5 and 4.4 kcal mol^{-1}, respectively). The larger activation barrier is associated with formation of the smaller cyclic structure (**IrIvy_ene**). Coordination of the double bond prior to C−H activation at the sp^2 carbon was proposed by Jones for C−H activation of benzene by Cp*Rh(PMe_3).[32] The coordination of the double bond in both cases is asymmetric, with a shorter

(31) Millan, A.; Bailey, P. M.; Maitlis, P. M. *J. Chem. Soc., Dalton Trans.* **1982**, 73.

(32) Jones, W. D.; Feher, F. J. *J. Am. Chem. Soc.* **1984**, *106*, 1650.

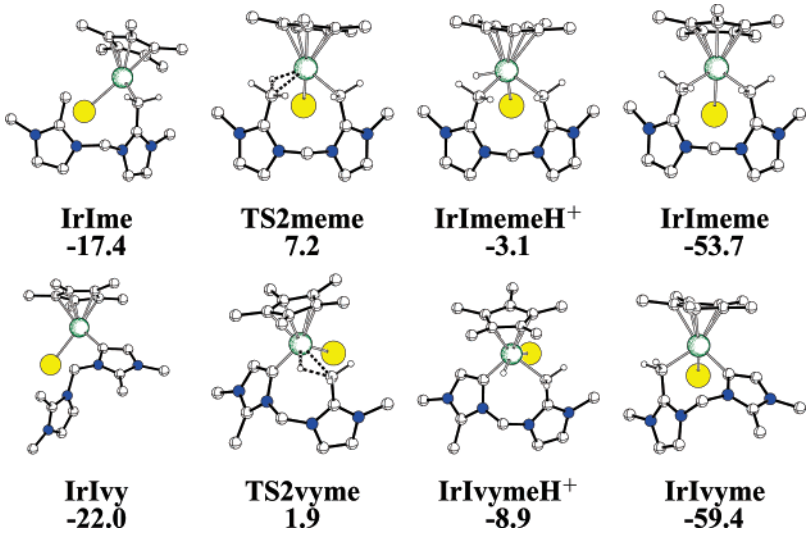

Figure 5. Optimized geometries and energies (kcal mol^{-1}, expressed relative to the reference system, see text) along the process for C−H activation at the methyl position from the intermediates **IrIme** (top) and **IrIvy** (bottom). Hydrogen atoms not involved in the reaction have been omitted for clarity. **IrImeme** and **IrIvyme** are monocationic, while the other complexes are dicationic.

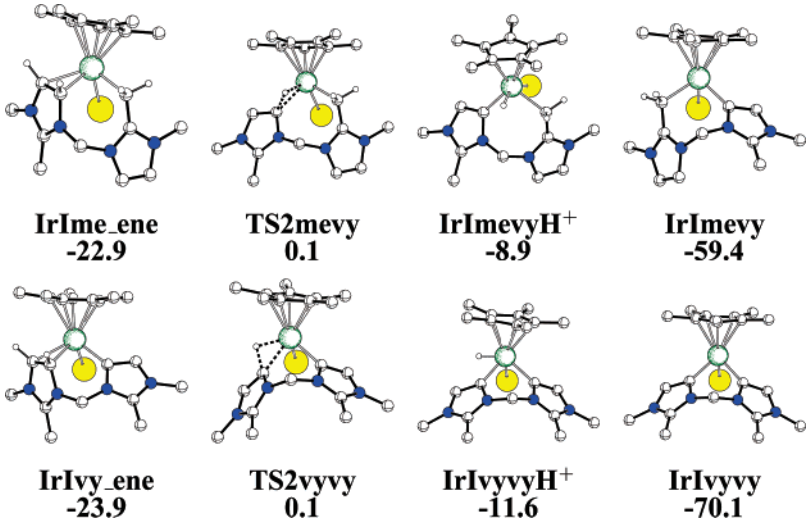

Figure 6. Optimized geometries and energies (kcal mol^{-1}, expressed relative to the reference system, see text) along the process for C−H activation at the C5 position from the intermediates **IrIme_ene** (top) and **IrIvy_ene** (bottom). Hydrogen atoms not involved in the reaction have been omitted for clarity. **IrImevy** and **IrIvyvy** are monocationic, while the other complexes are dicationic.

Ir−C5 bond than the Ir−C4 one (Ir−C4 = 2.229 Å, Ir−C5 = 2.164 Å, **IrIme_ene**; Ir−C4 = 2.253 Å, Ir−C5 = 2.148 Å, **IrIvy_ene**). This asymmetry is the result of the constraint associated with the presence of a linker between the two imidazole units. As a consequence of these geometrical features, the C−H activation is effective at the C5 position through **TS2mevy** and **TS2vyvy**, respectively (Figure 6). The activation barriers have very similar values (23 kcal mol^{-1}, **TS2mevy**; 24 kcal mol^{-1}, **TS2vyvy**) and are in the range found for other C−H activation processes.[17,28] The product of C−H activation featuring two abnormal carbenes, **IrIvyvyH**$^+$, is more acidic than **IrImevyH**$^+$ and **IrImemeH**$^+$, as illustrated by the larger exothermicity of the proton-transfer reaction to AcO^- (−58.5 kcal mol^{-1} vs −50.5 and −50.6 kcal mol^{-1}, respectively). This is a result of the stabilization of the 18-electron complex **IrIvyvy** by two strongly donating abnormal carbenes. The expected, but not observed, bis-abnormal carbene complex **IrIvyvy** is the thermodynamic product, and the two other isomers, **IrIvyme** and **IrImeme**, are lying higher in energy (10.7 and 16.4 kcal mol^{-1}, respectively).

Despite the strong thermodynamic preference for the bis-abnormal carbene, when expressed from the same reference, the energy values of all the intermediates and transition states for the transformations described are all negative or slightly positive (Figures 4−6), except for the transition states for the first C−H activation, **TS1me** and **TS1vy**. This first C−H activation step is thus the rate-determining step, and the calculated values point to an easier C−H activation at the methyl position. Thus under kinetic control the first metalation is at the methyl group and the calculations have shown that the second one is easier at the C5 position than at the other methyl. This second C−H activation, once **IrIme** has been formed, is both kinetically (**TS2mevy** lower than **TS2meme** by 7.1 kcal mol^{-1}) and thermodynamically (**IrImevy** more stable than **IrImeme** by 5.7 kcal mol^{-1}) favored to yield the mixed alkyl/abnormal carbene identical to the experimentally observed product **3**.

We also tested a pathway where the first metalation of the bisimidazolium **bisIm**$^{2+}$ occurs after the deprotonation of the ligand by the base. The monocationic species resulting from

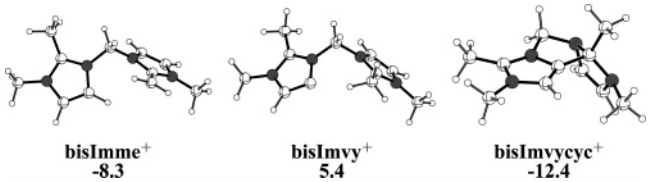

Figure 7. Optimized geometries and energies (kcal mol^{-1}, expressed relative to the reference system, see text) for the products of deprotonation of **bisIm**$^{2+}$ at the methyl position (left) and at the C5 position (middle), together with the product of cyclization (right).

deprotonation at the methyl position, **bisImme**$^{+}$, and at the C5 position, **bisImvy**$^{+}$, were optimized (Figure 7). In the case of the deprotonation at the methyl position, the reaction is exothermic by 8.3 kcal mol^{-1}, while in the case of deprotonation at C5, the reaction is endothermic by 5.4 kcal mol^{-1}. The greater acidity of the methyl group is explained by the stability of the base where conjugation of the "CH_2^-" group is achieved with the imidazolium ring, as illustrated by the perfect planar geometry for CH_2 and the ring (**bisImme**$^{+}$, Figure 7). Interestingly, the product of deprotonation at C5 easily evolves (activation barrier of 1.9 kcal mol^{-1}) to a cyclic structure, **bisImvycyc**$^{+}$ (Figure 7), resulting formally from nucleophilic attack of the abnormal carbene onto the C2 atom of the other imidazolium ring. The formation of this product is exothermic by 17.8 kcal mol^{-1} and would constitute a deactivation pathway for the abnormal carbene, had it been formed by deprotonation of the cationic bisimidazolium. However, we did not observe the formation of such product experimentally under the reaction conditions used and reacting **bisIm**$^{2+}$ in CH_3CN in the presence of an excess of NaOAc.

After deprotonation by the base, the ligand easily binds to Cp*IrI_2 to yield either **IrI$_2$me** or **IrI$_2$vy**, species from which the mechanism is similar to that already described. In that case, the first C−H activation that constituted the rate-determining step is bypassed, but the conclusions in terms of selectivity in the product obtained are identical. For the process starting with deprotonation at the methyl position, the highest point on the reaction pathway is the TS for the second C−H activation, **TS2mevy**, lying 8.4 kcal mol^{-1} above the entry channel {Cp*IrI_2 + **bisImme**$^{+}$}. For the process starting with deprotonation at C5, the entry channel is {Cp*IrI_2 + **bisImvycyc**$^{+}$} and the highest point along the reaction pathway is the opening of the cyclic structure to allow for coordination of **bisImvy**$^{+}$ at Ir and formation of **IrI$_2$vy**. The activation barrier is then 19.7 kcal mol^{-1}. Therefore, in the case where the first C−H bond breaking is due to deprotonation by the base, the calculations are also in agreement with the experimental results, and formation of **3** is kinetically preferred over the thermodynamic product **IrIvyvy**.

Formation of 6. The mechanism for the formation of the products **4** and **5** featuring a longer linker between the two imidazolium units has not been studied computationally. The three different products associated with the two C−H activation processes have been optimized, and the thermodynamic preference for the bis-abnormal complex is preserved. The latter is 11.8 kcal mol^{-1} more stable than the product featuring a mixed situation (activation at C5 and at the C2-Me group) and 19.4 kcal mol^{-1} more stable than the product featuring C−H activation at both C2-Me groups. These relative values are very similar to those observed with the methylene linker (10.7 and 16.4 kcal mol^{-1}, respectively), although the thermodynamic preference for the bis-abnormal isomer is slightly enhanced with the CH_2CH_2 linker.

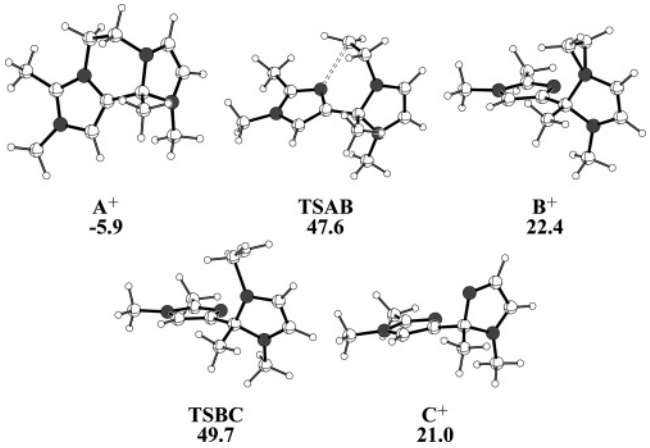

Figure 8. Optimized geometries and energies (kcal mol^{-1}, expressed relative to the reference system, which in the present case contains **bisImEt**$^{2+}$) for the intermediates and transition states located along the pathway for degradation of the ligand.

The deprotonation of the ligand 1,1′-ethylenebis(2,2′,3,3′-tetramethylimidazolium), **bisImEt**$^{2+}$, was studied computationally, and as in the case of the methylene linker, the deprotonation at the methyl, **bisImEtme**$^{+}$, is exothermic (−3.0 kcal mol^{-1}), whereas deprotonation at the C5 position, **bisImEtvy**$^{+}$, is endothermic (7.8 kcal mol^{-1}). As observed with the methylene linker, the deprotonation at C5 leads to a product, **A**$^{+}$, resulting from nucleophilic attack of C5 onto C2 of the other ring (Figure 8). The process is very facile (activation barrier of 3.4 kcal mol^{-1}) and exothermic (−16.7 kcal mol^{-1}). **A**$^{+}$ is 5.9 kcal mol^{-1} more stable than **bisImEtme**$^{+}$; a similar energy difference was observed between **bisImme**$^{+}$ and **bisImvycyc**$^{+}$ (4.1 kcal mol^{-1}). If deprotonation at the C5 position occurs, there is thus a thermodynamic preference for the cyclic structure.

From isomer **A**$^{+}$ the transition state corresponding to the rupture of one C−N bond, **TSAB**, has been located at 53.5 kcal mol^{-1} above **A**$^{+}$ (Figure 8). One of the C−N bonds with the CH_2CH_2 linker keeps a normal value (1.469 Å), while the other one is significantly elongated (2.519 Å). The product of this C−N bond cleavage, **B**$^{+}$, is an ethylene adduct on one nitrogen atom (Figure 8). This intermediate lies 28.3 kcal mol^{-1} above **A**$^{+}$. Dissociation of ethylene is effective once an activation barrier of 27.3 kcal mol^{-1} is surmounted in **TSBC**, leading to the product **C**$^{+}$ in an almost thermoneutral process (−1.4 kcal mol^{-1}). The C5−C2 bond in **C**$^{+}$ would be easily broken and the abnormal carbene at C5 is protonated, thus yielding 2 equiv of the ligand present in **6**. The activation barrier to form the ligand present in **6** from **A**$^{+}$ is high (53.5 kcal mol^{-1}), but the reaction is carried out in refluxing acetonitrile; thus this high barrier is expected to be overcome at this temperature. Moreover the reaction produces three molecules from one molecule, a process highly favored entropically at high temperature.

Conclusions

Scheme 4 shows a general overview of all the pathways tested computationally for the metalation of 1,1′-methylenebis-(2,2′,3,3′-tetramethylimidazolium) to Cp*IrI_2 in the presence of AcO^-. For each transformation, only the energy of the highest TS (numbers in red relative to the reference indicated by 0.0) has been given.

From the calculations it is difficult to conclude on the nature of the first metalation step, as the reaction conditions (refluxing acetonitrile) would allow surmounting activation barriers of ca. 30 kcal mol^{-1}. Nevertheless this point is not of crucial

Scheme 4. Simplified Mechanism for Formation of the Biscarbene Complexes from the Methylene-Bridged Bisimidazolium[a]

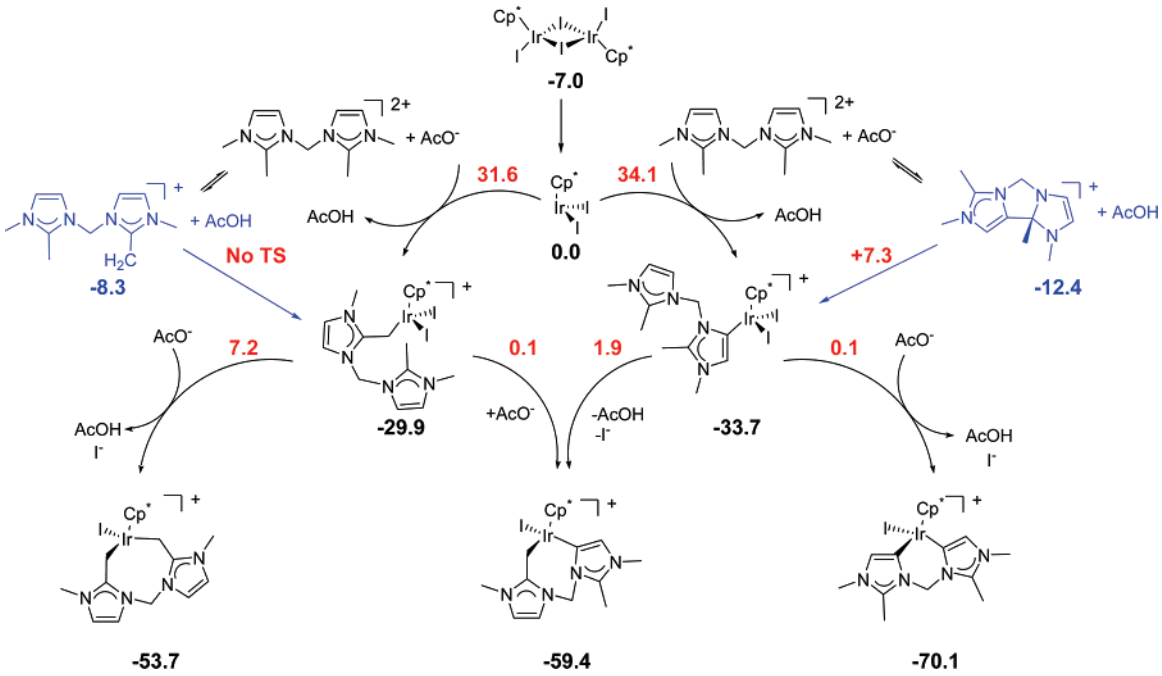

[a] The energy values (kcal mol^{-1}) for the highest TS along each path are given in red. In blue are given the energies of the products obtained after deprotonation of the bisimidazolium by the base.

importance, as both processes (direct ligand deprotonation or C−H activation) point to a kinetic preference at the C2-Me group. We recently reported that the role of the weak base in these systems may be different from the more generally accepted role of deprotonating the imidazolium salt prior to NHC formation.[17,18] The hydride formed after C−H activation is highly acidic and deprotonation by a weak base is easy.

For bisimidazolium salts, the action of the base may induce original reactivity as observed with the cyclic structure resulting from deprotonation at C5 (**bisImvycyc**$^+$, in Figure 7). Even though we did not observe such a compound experimentally, it may explain the degradation of the ligand in the case of the ethylene linker, the dimethylimidazole complex **6** being a consequence of this degradation. This illustrates the difficulty in designing a well-defined catalytic system, as the ligand may afford, according to reaction conditions, side reactions preventing the formation of the target compound. The present study also illustrates the sensitivity of bisimidazolium ions to attack by a base and, thus, the need, when possible, to use alternate routes for metalation.

For the Cp*IrI$_2$ fragment, C−H activation at the aliphatic position (C2-Me) is kinetically preferred over activation at the aromatic one (31.6 vs 34.1 kcal mol^{-1}). No precomplex (σ or π) could be located on the potential energy surface before the activation step. The difference in activation barrier reflects the difference in bond dissociation energy between the two different types of bonds (H−C(sp^3) vs H−C(sp^2)), and the relative energy of the products (after deprotonation, see Scheme 4) illustrates that in organometallic chemistry strong organic bonds lead to even stronger (relatively) metal−carbon bonds.[33] Once the first metalation has been produced, the second C−H activation is preferred kinetically at the aromatic C5 position. From **IrI$_2$me** the activation barrier at the aliphatic position is 7.1 kcal mol^{-1} higher than at the aromatic position (37.1 vs 30.0, Scheme 4). This could be explained by the size of the ring to be formed in the aliphatic C−H activation TS (eight-membered ring), while in the TS for activation at C5 a more stable seven-membered ring is formed. The differences are less important for the C−H activation from **IrI$_2$vy**, with the aromatic activation preferred over the aliphatic one by only 1.8 kcal mol^{-1} (33.8 vs 35.6 kcal mol^{-1}). In this case, formation of a six-membered ring is kinetically preferred over formation of a seven-membered ring.

The above results tend to indicate that C−H activation processes (aromatic/aliphatic) at Cp*Ir have similar activation barriers (ca. 30−35 kcal mol^{-1}), and activation at one or the other position might be critically influenced by the steric bulk of the metal fragment. When no orientating effect is effective, the activation of the aliphatic C−H bond is kinetically favored over aromatic activation with the Cp*IrI$_2$ fragment. The change in selectivity (aliphatic vs aromatic) observed for the second metalation is the result of an orientating effect of the already metalated imidazolium ring. The size of the ring to be formed is then a key factor influencing the kinetic preference. There is a larger energy difference between forming an eight- vs seven-membered ring (37.1 vs 30.0 kcal mol^{-1}) than between seven- and six-membered rings (35.6 vs 33.8 kcal mol^{-1}), showing that increasing the ring size is a destabilizing factor.

In conclusion, the calculations have rationalized the experimental results by showing that the first metalation is kinetically preferred at the aliphatic position. The second metalation process proceeds through a direct metal-mediated C−H activation, followed by deprotonation of the cationic metal-hydride with the base. This result clearly supports our previous suggestion that weak bases promote the metalation of imidazolium salts through irreversible C−H activation, thanks to the strongly exothermic deprotonation of the metal-hydride intermediate.[17,18] Cp*Ir(NHC) species are capable of a large variety of intra- or intermolecular and aromatic or aliphatic C−H activations. The factors determining the selectivity of these processes are influenced by electronic and steric parameters. Small changes within the bisimidazolium ligand provide great changes in the

(33) Clot, E.; Megret, C.; Eisenstein, O.; Perutz, R. N. *J. Am. Chem. Soc.* **2006**, *128*, 8350.

outcome of the reaction, hence leading to unexpected products. These observation may be helpful in the design of efficient Cp*Ir-based carbene complexes as catalysts for C−H activation processes.

Experimental Section

NMR spectra were recorded on Varian Innova 300 and 500 MHz spectrometers, using $CDCl_3$, acetone-d_6, and DMSO-d_6 as solvents. Elemental analyses were performed on an EA 1108 CHNS-O Carlo Erba analyzer. Electrospray mass spectra (ESI-MS) were recorded on a Micromass Quatro LC instrument; nitrogen was employed as the drying and nebulizing gas. 3-(2-Bromoethyl)-1-methylimidazolium bromide,[20] 1,2,3-trimethylimidazolium iodide,[34] and $[Cp^*IrCl_2]_2$[35] were synthesized according to literature procedures. All other reagents are commercially available and were used as received.

Synthesis of 1,1′-Ethylene-2,3,3′-trimethylbis(1*H*-imidazolium) Dibromide. 3-(2-Bromoethyl)-1-methylimidazolium bromide (1 g, 3.7 mmol) and 1,2-Dimethylimidazole (0.356 g, 3.7 mmol) were heated overnight at 110 °C in a high-pressure Shlenck without solvent. The reaction mixture was allowed to cool to room temperature. The product was extracted with CH_2Cl_2 as a white solid. Yield: 1.150 g, 85%. ^{1}H NMR (DMSO-d_6, 500 MHz): δ 9.32 (s, 1H, NC*H*N), 7.84, 7.73 (s, 2H, CH_{imid}), 7.62, 7.48 (d, $^3J_{H-H}$ = 1.99 Hz, 4H, CH_{imid}), 4.69−4.66 (m, 4H, C$H_{2linker}$), 3.84, 3.75 (s, 6H, N-CH_3), 2.61 (s, 3H, C-CH_3). ^{13}C{^{1}H} NMR (DMSO-d_6, 75 MHz): δ 146.04 (*C*-CH$_3$), 138.12 (N*C*HN), 124.31, 123.30, 123.23, 121.64 (*C*$_{imid}$), 48.41, 47.80 (*C*H$_{2linker}$), 36.71, 35.78 (N-*C*H$_3$), 10.71 (C-*C*H$_3$). Electrospray MS (20 V, *m*/*z*): 103.2 $[M]^{2+}$, 285.3 $[M + Br]^+$. Anal. Calcd for $C_{11}N_4H_{18}Br_2$ (mol wt 365.8): C, 36.09; H, 4.96; N, 15.30. Found: C, 36.12; H, 4.95; N, 15.32.

Synthesis of 1,1′-Methylenebis[(2,2′,3,3′-tetramethylimidazolium)] Diiodide. 1,2-Dimethylimidazole (1.5 g, 15.6 mmol) and diiodomethane (0.63 mL, 7.8 mmol) were heated at 110 °C in a high-pressure Shlenck without solvent for 12 h. The reaction mixture was allowed to cool to room temperature. The product was washed with CH_2Cl_2 to give the desired product as a brown solid. Yield: 3 g, 85%. ^{1}H NMR (DMSO-d_6, 300 MHz): δ 7.87, (d, $^3J_{H-H}$ = 2.30 Hz, 2H, CH_{imid}), 7.73 (d, $^3J_{H-H}$ = 2.30 Hz, 2H, CH_{imid}), 6.62 (s, 2H, C$H_{2linker}$), 3.76 (s, 6H, N-CH_3), 2.73 (s, 6H, C-CH_3). ^{13}C{^{1}H} NMR (DMSO-d_6, 75 MHz): δ 147.16 (*C*-CH$_3$), 123.83, 121.70 (*C*$_{imid}$), 57.54 (*C*H$_{2linker}$), 35.95 (N-*C*H$_3$), 11.21 (C-*C*H$_3$). Electrospray MS (30 V, *m*/*z*): 103.5 $[M]^{2+}$. Anal. Calcd for $C_{11}N_4H_{18}I_2$ (mol wt 460.10): C, 28.72; H, 3.94; N, 12.18. Found: C, 28.75; H, 4.10; N, 12.25.

Synthesis of 1,1′-Ethylenebis[(2,2′,3,3′-tetramethylimidazolium)] Dichloride. 1,2-Dimethylimidazole (1.5 g, 15.6 mmol) and 1,2-dichloroethane (0.61 mL, 7.8 mol) were heated at 110 °C in a high-pressure Shlenck for 15 h. The reaction mixture was allowed to cool to room temperature. The product was washed with CH_2Cl_2 and Et_2O. Yield: 1.200 g, 53%. ^{1}H NMR (DMSO-d_6, 300 MHz): δ 7.62, (s, 4H, CH_{imid}), 4.60 (s, 4H, C$H_{2linker}$), 3.76 (s, 6H, N-CH_3), 2.58 (s, 6H, C-CH_3). ^{13}C{^{1}H} NMR (DMSO-d_6, 75 MHz): δ 145.96 (*C*-CH$_3$), 123.20, 122.09 (*C*H$_{imid}$), 47.21 (*C*H$_{2linker}$), 35.62 (N-*C*H$_3$), 10.16 (C-*C*H$_3$). Electrospray MS (30 V, *m*/*z*): 110.5 $[M]^{2+}$. Anal. Calcd for $C_{12}N_4H_{20}Cl_2$ (mol wt 291.22): C, 49.49; H, 6.92; N, 19.24. Found: C, 49.52; H, 7.02; N, 19.36.

Synthesis of 1. Silver oxide (22 mg, 0.09 mmol) was added to a solution of 1,2,3-trimethylimidazolium iodide (45 mg, 0.18 mmol) in CH_2Cl_2. The solution was stirred at room temperature for 1 h, and then $[Cp^*IrCl_2]_2$ (75 mg, 0.09 mmol) was added. The mixture was stirred at 50 °C for 4 h and then filtered through Celite. The solvent was evaporated and the crude solid purified by column chromatography. The pure compound **1** was eluted with a mixture of dichloromethane/acetone (1:1) and precipitated in a mixture of CH_2Cl_2/hexanes to give an orange solid. Yield: 22%. ^{1}H NMR (300 MHz, $CDCl_3$): δ 6.47 (s, 1H, C*H* imidazole), 3.77 (s, 3H, N-CH_3), 3.56 (s, 3H, N-CH_3), 2.46 (s, 3H, C-CH_3), 1.57 (s, 15H, $C_5(CH_3)_5$). ^{13}C NMR (75 MHz, $CDCl_3$): δ 140.10 (*C*-Ir$_{abnormal}$), 128.99 (*C*-CH$_3$), 125.30 (*C*H), 87.14 (*C*$_5$(CH$_3$)$_5$), 36.50 (N-*C*H$_3$), 34.34 (N-*C*H$_3$), 10.66 (C-*C*H$_3$), 9.11 (C$_5$(*C*H$_3$)$_5$). Electrospray MS (15 V, *m*/*z*): 473.4 $[Cp^*IrLCl]^+$. Anal. Calcd for $C_{16}H_{25}N_2IrCl_2$: C, 37.79; H, 4.96; N, 5.51. Found: C, 36.17; H, 5.13; N, 5.13.

Synthesis of 2. A mixture of $[Cp^*IrCl_2]_2$ (200 mg, 0.25 mmol), 1,1′-ethylene-2,3,3′-trimethylbis(1*H*-imidazolium) dibromide (183 mg, 0.5 mmol), an excess of KBr, and NaOAc (62 mg, 0.75 mmol) was heated under reflux in CH_3CN (10 mL) for 12 h. After removing the solvent under reduced pressure, the crude solid was purified by column chromatography on silica gel using CH_2Cl_2/acetone (6:4) and KPF_6 as eluent. Recrystallization of this fraction from CH_2Cl_2/Et_2O afforded pure compound **2**. Yield: 16%. ^{1}H NMR ($CDCl_3$, 500 MHz): δ 7.01 (d, $^3J_{H-H}$ = 2.24 Hz, 1H, CH_{imid}), 6.91 (d, $^3J_{H-H}$ = 2.24 Hz, 1H, CH_{imid}), 6.26 (s, 1H, CH_{imid}), 4.75−4.70 (m, 1H, C$H_{2linker}$), 4.66−4.62 (dd, $^2J_{H-H}$ = 5.75 Hz, $^3J_{H-H}$ = 14.75 Hz, 1H, C$H_{2linker}$), 4.35−4.31 (dd, $^2J_{H-H}$ = 5.75 Hz, $^3J_{H-H}$ = 14.75 Hz, 1H, C$H_{2linker}$), 4.06−4.01 (m, 1H, C$H_{2linker}$), 3.81 (s, 3H, N-CH_3), 3.55 (s, 3H, N-CH_3), 2.44 (s, 3H, C-CH_3), 1.58 (s, 15H, C$_5$(CH_3)$_5$). ^{13}C{^{1}H} NMR ($CDCl_3$, 75 MHz): δ 152.68 (*C*-Ir), 141.88 (*C*-Ir$_{abnormal}$), 129.58, 123.80, 122.45 (*C*$_{imid}$), 119.64 (*C*-CH$_3$), 92.25 (*C*$_5$(CH$_3$)$_5$), 48.99, 47.61 (*C*H$_{2linker}$), 39.57, 34.12 (N-*C*H$_3$), 9.80 (C-*C*H$_3$), 9.39 (C$_5$(*C*H$_3$)$_5$). Electrospray MS (20V, *m*/*z*): 611 $[M]^+$. Anal. Calcd for $C_{21}N_4H_{31}IrPF_6Br$ (mol wt 756.58): C, 33.34; H, 4.13; N, 7.41. Found: C, 33.10; H, 3.92; N, 7.62.

Synthesis of 3. A mixture of $[Cp^*IrCl_2]_2$ (100 mg, 0.125 mmol), 1,1′-methylenebis[(2,2′,3,3′-tetramethylimidazolium)] diiodide (114.95 mg, 0.25 mmol), an exess of KI, and NaOAc (31 mg, 0.375 mmol) was heated under reflux in CH_3CN (10 mL) for 6 h. After removing the solvent under reduced pressure, the crude solid was purified by column chromatography on silica gel. Elution with CH_2Cl_2/acetone (3:7) and KPF_6 afforded the separation of compound **3**, which was recrystallized from CH_2Cl_2/Et_2O. Yield: 50%. ^{1}H NMR (acetone-d_6, 300 MHz): δ 7.40, (d, $^3J_{H-H}$ = 2.10 Hz, 1H, CH_{imid}), 7.16 (d, $^3J_{H-H}$ = 2.10 Hz, 1H, CH_{imid}), 6.47 (s, 1H, CH_{imid}), 6.30 (d, $^2J_{H-H}$ = 14.25 Hz, 1H, C$H_{2linker}$), 5.98 (d, $^2J_{H-H}$ = 14.25 Hz, 1H, C$H_{2linker}$), 4.23 (d, $^2J_{H-H}$ = 11.70 Hz, 1H, C-CH_2–Ir), 3.81 (s, 3H, N-CH_3), 3.77 (s, 3H, N-CH_3), 3.22 (d, $^2J_{H-H}$ = 11.70 Hz, 1H, C-CH_2-Ir), 2.95 (s, 3H, C-CH_3), 1.73 (s, 15H, C$_5$(CH_3)$_5$). ^{13}C{^{1}H} NMR (acetone-d_6, 75 MHz): δ 169.4 (*C*-CH$_2$-Ir), 146.02 (*C*-Ir$_{abnormal}$), 136.64 (*C*$_{imid}$), 132.83 (*C*-CH$_3$), 126.39, 122.74 (*C*$_{imid}$), 93.80 (*C*$_5$(CH$_3$)$_5$), 62.47 (*C*H$_{2linker}$), 41.33, 38.87 (N-*C*H$_3$), 14.52 (*C*-CH$_3$), 13.76 (C$_5$(*C*H$_3$)$_5$), −15.64 (C-*C*H$_2$-Ir) (assignment of ^{13}C-{^{1}H} NMR signals is confirmed by ^{13}C−^{1}H inverse correlation). Electrospray MS (30 V, *m*/*z*): 659.5 $[M]^+$, 266.3 $[M - I]^{2+}$. Anal. Calcd for $C_{21}N_4H_{31}IrPF_6I$ (mol wt 803.58): C, 31.39; H, 3.89; N, 6.97. Found: C, 31.42; H, 3.90; N, 6.99.

Synthesis of 4, 5, and 6. A mixture of $[Cp^*IrCl_2]_2$ (200 mg, 0.25 mmol), 1,1′-ethylenebis[(2,2′,3,3′-tetramethylimidazolium)] dichloride (146 mg, 0.5 mmol), and NaOAc (62 mg, 0.75 mmol) was heated at reflux in CH_3CN (10 mL) for 36 h. The suspension was filtered through Celite to remove insoluble salts and unreacted ligand. The solution was concentrated under reduced pressure. The crude solid was redissolved in dichloromethane and purified by column chromatography using silica gel. Elution with CH_2Cl_2/acetone (8:2) afforded the separation of a yellow band. Recrystallization of this fraction from CH_2Cl_2/hexane mixtures afforded pure compound **6**. Yield: 15%. Subsequent elution with gradient CH_2Cl_2/acetone (6:4) and KPF_6 gave the separation of a second intense

(34) Ricciardi, F.; Romanchick, W. A.; Joullie, M. M. *J. Polym. Sci. Polym. Chem.* **1983**, *21*, 1475.

(35) Ball, R. G.; Graham, W. A. G.; Heinekey, D. M.; Hoyano, J. K.; McMaster, A. D.; Mattson, B. M.; Michel, S. T. *Inorg. Chem.* **1990**, *29*, 2023.

Table 1. Crystallographic Data.

	2	3	5	6
empirical formula	$C_{22}H_{32}Cl_3F_6IrPBrN_4$	$C_{21}H_{31}N_4IrPF_6I.CH_2Cl_2$	$C_{24}H_{35}Cl_7F_6IrPN_4$	$C_{15}H_{23}Cl_2IrN$
fw	875.95	888.49	964.88	494.45
wavelength (Å)	0.71073	0.71073	0.71073	0.71073
temperature (K)	293(2)	293(2)	293(2)	293(2)
cryst syst	monoclinic	monoclinic	monoclinic	monoclinic
space group	*P*2(1)	*P*2(1)/*n*	*C*2/*c*	*P*2(1)/*c*
a (Å)	11.2711(9)	12.3869(6)	38.213(2)	7.4921(4)
b (Å)	9.1727(8)	15.5378(7)	8.3789(5)	16.5039(9)
c (Å)	14.3367(11)	15.7627(7)	23.3134(15)	13.9741(8)
α (deg)	90	90	90	90
β (deg)	90.512(2)	102.1020(10)	102.6080(10)	101.7040(10)
γ (deg)	90	90	90	90
V (Å^3)	1482.2(2)	2966.3(2)	7284.5(8)	1691.96(16)
Z	2	4	8	4
density (calcd) (Mg/m^3)	1.963	1.989	1.760	1.941
absorp coeff (mm^{-1})	6.235	5.833	4.277	8.199
no. of reflns collected	8409	20 253	3776	13 751
goodness of fit on R^2	1.014	1.013	1.033	1.030
final *R* indices	R1 = 0.0506	R1 = 0.0243	R1 = 0.0414	R1 = 0.0369
[$I > 2\sigma(I)$]	wR2 = 0.0834	wR2 = 0.0584	wR2 = 0.1099	wR2 = 0.0691

orange band. Further elution with a mixture of CH_2Cl_2/acetone (4:6) and KPF_6 afforded the separation of a third yellow band that contains **5**. Recrystallization from CH_2Cl_2/Et_2O gave pure **5**. Yield: 30%.

The second band was redissolved in dichloromethane and purified again by column chromatography on silica gel using a mixture of CH_2Cl_2/acetone (5:5) and KPF_6. Recrystallization from CH_2Cl_2/Et_2O gave pure **4** as an orange oil. Yield: 12%.

Characterization of 4. ^{1}H NMR ($CDCl_3$, 300 MHz): δ 7.13 (d, $^3J_{H-H}$ = 2.00 Hz, 1H, C*H*$_{imid}$), 6.96 (d, $^3J_{H-H}$ = 2.00 Hz, 1H, C*H*$_{imid}$), 6.30 (s, 1H, C*H*$_{imid}$), 4.84−4.76 (m, 1H, C*H*$_{2linker}$), 4.70−4.63 (dd, $^2J_{H-H}$ = 5.50 Hz, $^3J_{H-H}$ = 14.55 Hz, 1H, C*H*$_{2linker}$), 4.45−4.38 (dd, $^2J_{H-H}$ = 5.50 Hz, $^3J_{H-H}$= 14.55 Hz, 1H, C*H*$_{2linker}$), 4.17−4.10 (m, 1H, C*H*$_{2linker}$), 3.88 (s, 3H, N-C*H*$_3$), 3.72 (d, $^2J_{H-H}$ = 13.65 Hz, 1H, C-C*H*$_2$-Ir), 3.61 (s, 3H, N-C*H*$_3$), 2.60 (d, $^2J_{H-H}$ = 13.65 Hz, 1H, C-C*H*$_2$-Ir), 2.48 (s, 3H, C-C*H*$_3$), 1.63 (s, 15H, $C_5(CH_3)_5$). ^{13}C{^{1}H} NMR ($CDCl_3$, 75 MHz): δ 153.98 (*C*-CH$_2$-Ir), 142.09 (*C*-Ir$_{abnormal}$), 127.42, 123.92, 122.17 (*C*H$_{imid}$), 121.50 (*C*-CH$_3$), 92.05 ($C_5(CH_3)_5$), 49.18, 47.27 (*C*H$_{2linker}$), 38.19, 34.13 (N-*C*H$_3$), 29.89 (C-*C*H$_2$-Ir), 9.83 (C-*C*H$_3$), 9.20 ($C_5(CH_3)_5$). Electrospray MS (20 V, *m*/*z*): 581.3 [M]$^+$, 547.3 [M − Cl + H]$^+$. Anal. Calcd for $C_{22}N_4H_{33}ClIrPF_6$ (mol wt 726.16): C, 36.39; H, 4.58; N, 7.72. Found: C, 36.32; H, 4.40; N, 7.70.

Characterization of 5. ^{1}H NMR ($CDCl_3$, 500 MHz): δ 6.39 (s, 2H, C*H*$_{imid}$), 4.84−4.76 (m, 2H, C*H*$_{2linker}$), 4.25−4.39 (m, 2H, C*H*$_{2linker}$), 3.58 (s, 6H, N-C*H*$_3$), 2.54 (s, 6H, C-C*H*$_3$), 1.62 (s, 15H, $C_5(CH_3)_5$). ^{13}C{^{1}H} NMR ($CDCl_3$, 125 MHz): δ 141.09 (*C*-Ir$_{abnormal}$), 129.36 (*C*-CH$_3$), 126.19 (*C*$_{imid}$), 90.55 ($C_5(CH_3)_5$), 46.95 (*C*H$_{2\ inker}$), 34.13 (N-*C*H$_3$), 9.94 (C-*C*H$_3$), 9.25 ($C_5(CH_3)_5$). Electrospray MS (20 V, *m*/*z*): 581.3 [M]$^+$. Anal. Calcd for $C_{22}N_4H_{33}IrPF_6Cl$ (mol wt 726.16): C, 36.39; H, 4.58; N, 7.72. Found: C, 36.40; H, 4.36; N, 7.62.

Characterization of 6. ^{1}H NMR ($CDCl_3$, 300 MHz): δ 7.33 (d, $^3J_{H-H}$ = 1.6 Hz, 2H, C*H*$_{imid}$), 6.74 (d, $^3J_{H-H}$ = 1.6 Hz, 2H, C*H*$_{imid}$), 3.60 (s, 3H, N-C*H*$_3$), 2.66 (s, 3H, C-C*H*$_3$), 1.63 (s, 15H, $C_5(CH_3)_5$). ^{13}C{^{1}H} NMR ($CDCl_3$, 125 MHz): δ 148.5 (*C*-CH$_3$), 129.41, 120.24 (*C*$_{imid}$), 84.95 ($C_5(CH_3)_5$), 34.06 (N-*C*H$_3$), 29.64 (C-*C*H$_3$), 9.09 ($C_5(CH_3)_5$). Electrospray MS (20 V, *m*/*z*): 459.1 [M − Cl]. Anal. Calcd for $C_{15}N_2H_{23}IrCl_2$ (mol wt 494.48): C, 36.43; H, 4.69; N, 5.67. Found: C, 36.42; H, 4.60; N, 5.60.

X-ray Diffraction Studies. Crystals for suitable X-ray diffraction of **2**, **3**, **5**, and **6** were obtained by slow diffusion of ether in a concentrated solution of the compound in CH_2Cl_2.

Crystal data are summarized in Table 1. Data collection was performed at room temperature on a Siemens Smart CCD diffractometer using graphite-monochromated Mo Kα radiation (λ = 0.71073 Å). The diffraction frames were integrated using the SAINT package.

Space group assignment was based on systematic absences, E statistics, and successful refinement of the structures. The structures were solved by direct methods with the aid of successive difference Fourier maps and were refined using the SHELXTL 6.1 software package. All non-hydrogen atoms were refined anisotropically, and hydrogen atoms were assigned to ideal positions and refined using a riding model.

Computational Details. The calculations were performed with the Gaussian03 package[36] at the B3PW91 level.[37] Iridium was represented by the relativistic effective core potential (RECP) from the Stuttgart group and the associated basis set (SDDALL keyword in Gaussian03),[38] augmented by an f polarization function (α = 0.95).[39] Iodine was represented by the relativistic effective core potential (RECP) from the Stuttgart group and the associated basis set (SDDALL keyword in Gaussian03),[40] augmented by a d polarization function (α = 0.289).[41] A 6-31G(d,p) basis set was used for all the other atoms (C, N, H, O).[42] Corrections for basis set superposition errors were not considered, as this work deals essentially with comparison of behavior between two different sites in the same molecule and not with accurate determination of interaction energies between different molecules.

The geometry optimizations were performed without any symmetry constraint followed by analytical frequency calculations to confirm that a minimum or a transition state had been reached. The nature of the species connected by a given transition state structure was checked by optimization as minima of slightly altered TS geometries along both directions of the transition state vector. The energies of all the systems studied at the B3PW91 level in the gas phase were computed with inclusion of solvent effects (acetonitrile) according to the PCM scheme as implemented in Gaussian.[43]

(36) Pople, J. A.; et al. *Gaussian 03*, Revision C.02; 2003.
(37) Becke, A. D. *J. Chem. Phys.* **1993**, *98*, 5648.
(38) Andrae, D.; Haussermann, U.; Dolg, M.; Stoll, H.; Preuss, H. *Theor. Chim. Acta* **1990**, *77*, 123.
(39) Ehlers, A. W.; Bohme, M.; Dapprich, S.; Gobbi, A.; Hollwarth, A.; Jonas, V.; Kohler, K. F.; Stegmann, R.; Veldkamp, A.; Frenking, G. *Chem. Phys. Lett.* **1993**, *208*, 111.
(40) Bergner, A.; Dolg, M.; Kuchle, W.; Stoll, H.; Preuss, H. *Mol. Phys.* **1993**, *80*, 1431.
(41) Hollwarth, A.; Bohme, M.; Dapprich, S.; Ehlers, A. W.; Gobbi, A.; Jonas, V.; Kohler, K. F.; Stegmann, R.; Veldkamp, A.; Frenking, G. *Chem. Phys. Lett.* **1993**, *208*, 237.
(42) Hariharan, P.; Pople, J. A. *Theor. Chim. Acta* **1973**, *28*, 213.
(43) Tomasi, J.; Mennucci, B.; Cammi, R. *Chem. Rev.* **2005**, *105*, 2999.

The geometries obtained in the gas phase were used without further reoptimization within the PCM methodology, and the united atom topological model with UAKS radii was used.

Acknowledgment. We gratefully acknowledge financial support from the MEC of Spain (CTQ2005-05187), Bancaixa (P1.1B2004-07), the CNRS, and the MESR. R.C. and M.F. thank the Spanish Ministerio de Educación y Ciencia for a fellowship, and J.A.M. thanks the Ramón y Cajal Program.

Supporting Information Available: X-ray crystallographic files in CIF format for the structure determinations of **2**, **3**, **5**, and **6**, a complete reference for Gaussian 03, and DFT-computed Cartesian coordinates for the optimized molecules and their PCM electronic energies. This material is available free of charge vie the Internet at http://pubs.acs.org.

OM7006979